ELSEVIER

Catalysis Today 63 (2000) 53–62

CATALYSIS TODAY

www.elsevier.com/locate/cattod

Acid–base properties and active site requirements for elimination reactions on alkali-promoted MgO catalysts

V.K. Díez, C.R. Apesteguía, J.I. Di Cosimo*

Instituto de Investigaciones en Catálisis y Petroquímica (INCAPE), UNL-CONICET, Santiago del Estero 2654, 3000 Santa Fe, Argentina

Received 28 October 1999; accepted 20 February 2000

Abstract

Base-catalyzed elimination reactions were studied on MgO and alkali-modified MgO catalysts using 2-propanol as a probe reactant. The effect of the acid–base properties on the catalyst activity and selectivity was investigated by modifying the surface properties of MgO with 1 mol% of alkaline metals. Group IA metals promote the formation of medium- and high-strength basic sites, thereby increasing the basic site density and strength. The addition of alkaline promoters improves the MgO activity for 2-propanol conversion reactions. The selectivity toward dehydration or dehydrogenation products depends on the base site nature, so that intermediate-strength base sites promote acetone formation, whereas high-strength base sites selectively yield propylene. 2-Ppropanol decomposition to acetone and propylene is proposed to take place via an E_{1cB} mechanism in two parallel pathways sharing a common 2-propoxy intermediate.

Keywords: 2-Propanol; Base catalysis; Elimination reactions

1. Introduction

Alkaline earth metal oxides are active and selective solid base catalysts in a variety of organic reactions involving formation of carbanion intermediates. Particularly, MgO-based catalysts have shown to promote several base-catalyzed reactions such as double bond isomerization [1], aldol condensation [2,3], Knoevenagel condensations [4] and alcohol coupling [5].

Deposition of metal cations on MgO-based catalysts for producing new centers with different acid–base properties have been reported in the literature. Kurokawa et al. [6] reported that promotion of MgO with several cations such as Ni^{2+}, Cu^{2+}, Fe^{3+}, Cr^{3+}, increases the basic properties and the catalytic activity for 2-propanol dehydrogenation. Malinowski [7] showed that the changes on the acid–base properties of MgO induced by promotion with alkaline cations depend on both the amount and the kind of the cation. Furthermore, in previous work, we found [3] that the addition of 1 wt.% alkaline or alkaline earth metals to MgO increases the electrodonating properties of MgO and as a consequence, increases also its catalytic activity for the oligomerization of acetone.

Characterization of metal oxides by direct measurements of acidity or basicity adsorbing gaseous probe molecules have been widely reported in the literature [8]. Several catalytic test reactions have been also used for indirect characterization of the catalyst acidity in reaction conditions. In contrast, very few have been employed as a catalytic probe for determining catalysts basicity [8]. Among them we can mention decomposition of alcohols such as 2-propanol [9,10], 2-methyl-3-butyn-2-ol [11,12], 2-methyl-2-butanol

* Corresponding author. Tel.: +54-342-4555279; fax: +54-342-4531068.
E-mail address: dicosimo@fiqus.unl.edu.ar (J.I. Di Cosimo).

0920-5861/00/$ – see front matter
PII: S0920-5861(00)00445-4

[13] and cyclohexanol [14]. Nevertheless, the use of reliable test reactions for characterizing the catalyst basicity is still a matter of controversy in the literature [9,10,12,15].

Decomposition of 2-propanol has been widely employed to investigate the catalyst acid–base properties of alkaline earth-based catalysts [6,16,17]. 2-Propanol decomposes via elimination reactions such as dehydrogenation and dehydration that can proceed through different mechanisms depending on the acid–base nature of the catalysts. It is generally accepted that strong solid acids dehydrate 2-propanol to the olefin in an E_1 mechanism in which only the acidic sites take part, whereas on amphoteric oxides the reaction leads to ether and in a concerted E_2 mechanism occurring on acid–base pairs, to olefin [15]. However, dehydration can also take place on strongly basic catalysts containing acid–base pairs of imbalanced strength through an E_{1cB} mechanism [15]. On the other hand, the dehydrogenation reaction proceeds in relevant extent only on strongly basic catalysts [16,17].

In this work we prepared a set of MgO-based catalysts promoted with 1 mol% of alkaline metals (Li^+, Na^+, K^+ and Cs^+). We characterized the basic properties of these materials by CO_2 adsorption using a variety of physical and spectroscopic techniques. Our aim was to investigate the effect of the alkali promotion on the chemical nature, density, strength and strength distribution of the basic sites present on the MgO surface.

We use the decomposition of 2-propanol to establish the site requirements for dehydrogenation and dehydration elimination reactions. The rates and product distribution for 2-propanol reactions depend on the catalyst surface acid–base properties. Our goal was to elucidate the role of the surface active sites on the sequential pathways required for elimination reactions on MgO-based catalysts.

2-Propanol decomposes via elimination reactions that are often included in the reaction mechanism of important industrial processes. Hydrogen and water-abstraction pathways, for example, are involved in the mechanisms of industrial processes such as aldol condensation of aldehydes and ketones, and linear alcohol coupling to branched higher alcohols.

Catalytic and mechanistic information gained using 2-propanol decomposition is useful not only for characterizing surface acid–base properties but also for elucidating elimination reaction pathways, especially on metal oxide catalysts.

2. Experimental

2.1. Catalyst preparation

A high surface area MgO was prepared by rehydration at room temperature of commercial MgO (Carlo Erba, 99%, 27 m^2/g) with distilled water, as described elsewhere [3]. The obtained $Mg(OH)_2$ was thermally decomposed in N_2 at 773 K. A set of alkali-promoted A/MgO samples (A = Li, Na, K or Cs) was prepared by impregnation. The alkali metal A was added to MgO using a hydroxide aqueous solution that contained the required A concentration to obtain about 1 mol% A. After impregnation, the hydrated samples were dried at 353 K and decomposed in N_2 at 773 K.

2.2. Catalyst characterization

The chemical content of promoter A was analyzed by atomic absorption spectrometry (AAS). BET surface areas (S_g) were determined by N_2 adsorption at 77 K in a Nova-1000 Quantachrom sorptometer.

The CO_2 chemisorption was carried out at room temperature in a conventional glass vacuum apparatus equipped with an MKS Baratron pressure gauge. The amount of irreversibly held CO_2 was calculated by the double-isotherm method [3] as the difference between total and weakly adsorbed CO_2. The pressure range of isotherms was 0–20 kPa. Catalysts were previously outgassed at 773 K in a vacuum of 8×10^{-6} kPa.

CO_2 binding energies were determined by temperature-programmed desorption (TPD) of CO_2 pre-adsorbed at room temperature. Samples were pre-treated in situ in flowing N_2 at 773 K, cooled down to room temperature and then exposed to a flowing mixture of 2% CO_2 in N_2 until surface saturation. Weakly bonded CO_2 was removed by flushing with N_2 and temperature was then raised at 8 K/min up to 773 K. Desorbed CO_2 was converted in CH_4 before analysis by FID.

The chemical nature of adsorbed surface CO_2 species was determined by infrared spectroscopy (IR) after CO_2 adsorption at room temperature and sequential evacuation at increasing temperatures.

Spectra were taken at room temperature using an inverted T-shaped cell fitted with CaF_2 windows and containing the sample pellet. Data were collected at room temperature in an FTIR 8500 Shimadzu spectrometer. The absorbance scales were normalized to 50 mg pellets.

2.3. Catalytic tests

The 2-propanol decomposition was carried out at 533 K and 100 kPa in a differential fixed-bed tubular reactor. The reactant was introduced as 1:15 2-propanol/N_2 mixture. Samples were pre-treated in situ in flowing N_2 at 773 K for 1 h to remove water and carbon dioxide. Typical space velocities (WHSV) were $2\,h^{-1}$. Reaction products were analyzed by on-line GC in a Varian Star 3400 CX chromatograph equipped with an FID and a Porapak R column. Data were collected every 20 min for 10 h. Reaction products were acetone (C_3one) and propylene (C_3=).

3. Results and discussion

3.1. Density and strength distribution of the basic sites

Table 1 presents the physicochemical properties of pure MgO and alkali-promoted A/MgO samples. The alkali metal loading was in all cases about 1 mol%. Promotion of MgO with group IA metals decreases the catalyst surface area, probably because of metal hydroxide melting and pore blocking during preparation procedures.

The basicity of an oxide surface is generally related to the electrodonating properties of the combined oxygen anions, so that the higher the partial negative charge on the combined oxygen anions, the more basic the oxide. The oxygen partial negative charge ($-q_o$) would reflect, therefore, the electron donor properties of the oxygen in single-component oxides. The $-q_o$ values of A_2O promoter oxides, as calculated from the electronegativity equalization principle [18], are shown in Table 1. It is observed that $-q_o$ is higher on A_2O oxides as compared to MgO, thereby indicating that promotion with more basic A_2O oxides may probably increase the basicity of pure MgO.

The number of basic sites available for the irreversible CO_2 adsorption at room temperature is presented in Table 1. Langmuir-type adsorption isotherms were obtained for the irreversible CO_2 adsorption on all the A/MgO samples. We measured a value of 1.83 μmol/m^2 for unpromoted MgO, whereas Auroux and Gervasini [19] reported a value of 1.45 μmol/$m^2$and Philipp and Fujimoto [20] found 4.31 μmol/m^2 using similar gaseous volumetry technique for pure MgO. Furthermore, a measure of the number and strength distribution of basic sites on MgO and A/MgO catalysts was obtained by TPD of CO_2 adsorbed at room temperature (Fig. 1). Total evolved CO_2 values (n_{CO_2}) were determined from the area under the curves of Fig. 1 and are reported in Table 1. The n_{CO_2} values compared favorably with the irreversible CO_2 adsorption measurements,

Table 1
Physicochemical properties of MgO and A/MgO catalysts: chemical composition, BET surface areas and CO_2 adsorption results

Catalyst A/MgO	$-q_o$ in A_2O	Metal A ionic radius (Å)	Metal A loading[a] (mol%)	S_g (m^2/g)	Irreversible CO_2 chemisorption (μmol/m^2)	TPD of adsorbed CO_2			
						Desorption peaks (area %)			n_{CO_2} (μmol/m^2)
						L	M	H	
MgO	0.50[b]	0.66[c]	–	125	1.83	18.2	58.0	23.8	2.33
Li/MgO	0.80	0.68	0.92	134	2.14	22.3	59.5	18.2	3.44
Na/MgO	0.81	0.97	1.04	94	1.96	16.3	57.1	26.6	2.52
K/MgO	0.89	1.33	0.84	83	2.11	19.4	49.9	30.7	2.96
Cs/MgO	0.94	1.67	0.82	70	2.23	16.3	40.4	43.3	3.73

[a] By AAS.
[b] In MgO.
[c] Mg^{2+}.

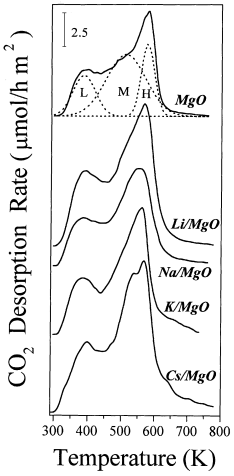

Fig. 1. TPD of CO_2 on MgO and A/MgO catalysts.

although the latter values are lower than the former ones due to the evacuation procedure used in the double-isotherm method. Using CO_2 TPD, McKenzie et al. [21] reported a value of 4.4 μmol/m^2, whereas Kurokawa et al. [22] measured 2.4 μmol/m^2 for pure MgO. Although the differences in sample preparation procedures and measuring techniques, the present results of either CO_2 chemisorption or TPD agree reasonably with literature data.

Both the n_{CO_2} and the irreversible CO_2 chemisorption values on unpromoted MgO are lower than those obtained on A/MgO samples, probably because the higher total surface cation content in A/MgO oxides increases the MgO basic site density. The amount of new sites generated by alkali promotion increases proportionally to the electrodonating character of the promoter oxide, with the exception of Li, which generates more basic sites than the expected. Kanno and Kobayashi [23] characterized a series of alkali-promoted MgO samples by TPD and IR of CO_2 and reported that the Li generates more and stronger basic sites than the other metals of the group IA. Similarly, in a previous work on the synthesis of isophorone by aldol condensation of acetone over 1 wt.% alkali/MgO [3], we found that the basic site density as well as the catalytic activity and selectivity are much higher on the Li/MgO sample as compared to the other series members. We attributed this distinctive behavior to an ionic size effect since the matching ionic radius of Li^+ and Mg^{2+} cations would entitle Li^+ to cause not only surface but also structural promotion of the MgO lattice.

This increase of the number of basic sites upon alkali promotion has been previously reported in the literature and seems to depend not only on the electrodonating properties of the promoter but also on its loading [23,24]. In fact, we reported [3] that 1 wt.% of alkali metals substantially increases the basic site density of pure MgO and that the generation of new basic sites is enhanced at higher molar loading of promoter A.

The structure of chemisorbed CO_2 species was determined by IR measurements of pre-adsorbed CO_2. Fig. 2 presents the IR spectra obtained on MgO and Li/MgO catalysts after CO_2 adsorption and sequential evacuation at 298, 373, 473 and 573 K. Three surface species of adsorbed CO_2 were detected on MgO: bicarbonate, unidentate and bidentate carbonates [20,25–27]. These species were detected also in

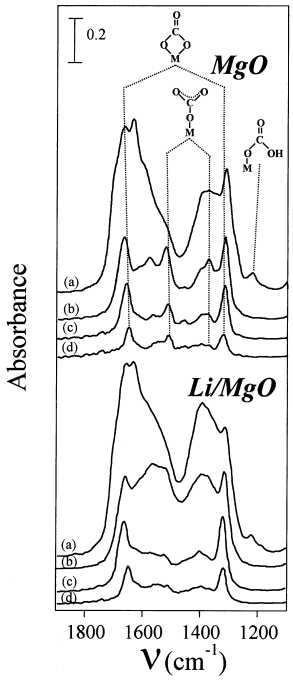

Fig. 2. Infrared spectra of CO_2 adsorbed on MgO and Li/MgO catalysts upon desorption at increasing evacuation temperatures: (a) 298 K, (b) 373 K, (c) 473 K, (d) 573 K.

all the A/MgO samples with similar qualitative spectra after CO_2 evacuation at increasing temperatures. The different CO_2 adsorption modes reveal that the surface of MgO or A/MgO oxides contain oxygen atoms of different chemical nature. Unidentate carbonate formation requires isolated surface O^{2-} ions, i.e., low-coordination anions, such as those present in corners or edges and exhibits a symmetric O–C–O stretching at 1360–1400 cm^{-1} and an asymmetric O–C–O stretching at 1510–1560 cm^{-1}. Bidentate carbonate forms on Lewis-acid–Brönsted-base pairs (M^{n+}–O^{2-} pair site, where M^{n+} is the metal cation Mg^{2+} or A^{+}), and shows a symmetric O–C–O stretching at 1320–1340 cm^{-1} and an asymmetric O–C–O stretching at 1610–1630 cm^{-1}. Bicarbonate species formation involves surface hydroxyl groups. Bicarbonates show a C–OH bending mode at 1220 cm^{-1} as well as a symmetric and an asymmetric O–C–O stretching at 1480 and 1650 cm^{-1}, respectively.

Bicarbonate is the most labile species and disappears after evacuation at 373 K. Contrarily, both the unidentate and bidentate carbonates remain on the surface after evacuation at 573 K, however, only the unidentate bands are observed upon evacuation at higher temperatures. These results suggest the following strength order for surface basic sites: O^{2-} ions > oxygen in Mg(A)–O pairs > OH groups.

After evacuation at room temperature, the intensities of the bidentate carbonate bands in all the samples are stronger than those of the unidentate bands (Fig. 2), thereby indicating a predominant contribution of the Mg(A)–O pairs to the total basicity.

In order to quantify the contribution of the different surface species to the total density of basic sites, deconvolution of the CO_2 TPD profiles was performed. The TPD profiles of Fig. 1 were decomposed in three desorption bands, i.e., low temperature peak (L), middle temperature peak (M) and high temperature peak (H). Based on the IR results, these peaks are assigned to low- (OH groups), medium- (Mg–O pairs with a probably small contribution of A–O pairs) and high-strength (O^{2-} ions) basic sites, respectively. The CO_2 TPD deconvolution results are shown in Table 1. In agreement with the IR results, MgO and A/MgO catalysts activated at 773 K contain predominantly medium-strength basic sites, i.e., oxygen in Mg(A)–O pairs, which represent 40–60% of the total base site density.

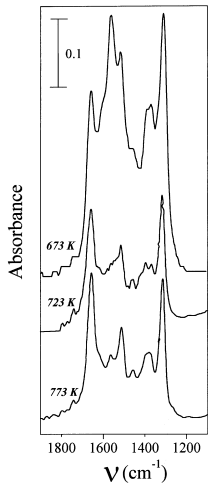

Fig. 3. Infrared spectra of CO_2 adsorbed on MgO calcined at different temperatures.

However, the fact that the medium-strength sites prevail on the surface of MgO-based catalysts seems to depend on the sample activation procedure. Fig. 3 shows the IR spectra obtained on three MgO wafers activated in situ at 673, 723 and 773 K, after CO_2 adsorption at room temperature and evacuation at 473 K. It can be observed in Fig. 3 that the bands attributed to the unidentate carbonate are more intense than those of the bidentate carbonate at a pre-treatment temperature of 673 K, but they are depleted as the calcination temperature increases. In fact, the intensity ratio defined as the intensity of the asymmetric stretching of the bidentate carbonate/intensity of the asymmetric stretching of the unidentate carbonate presented values of 0.8, 1.4 and 1.6 at 673, 723 and 773 K, respectively. Furthermore, we have previously reported [25] that a MgO sample activated at 673 K contains about 60% of high-strength basic sites in contrast to the 24% reported in Table 1 for the sample activated at 773 K.

In previous work by Morterra et al. [26] on $MgAl_2O_4$ and by Evans and Whateley [27] on MgO, these authors investigated by IR of CO_2 the role of surface hydroxylation on the generation of strong basic sites. They concluded that the strong basicity, responsible for unidentate carbonate formation, is promoted by the presence of surface OH groups. Our results show that the unidentate/bidentate intensity ratio decreases with increasing the pre-treatment

temperature and it is accompanied by a reduction of the surface area. Then, the loss of unidentate carbonate formation centers (low coordination surface O^{2-} ions) can be ascribed to both the elimination of surface defects and the enhancement of the surface dehydroxylation at high activation temperatures.

The effect of the electrodonating properties of the promoter oxide on the base site strength was also investigated. Table 1 shows that, whereas, the relative contribution of the L-peak remains almost unchanged, the area % of the H-peak clearly increases with increasing $-q_o$ at expenses of the M-peak. Thus, the higher the electron donor properties of the promoter oxide, the higher the generation of the strongest basic sites. For example, the amount of high-strength basic sites (H-peak) on Cs/MgO sample is 1.61 μmol/m^2, which is a value three times higher than that measured on pure MgO (0.55 μmol/m^2). The enhancement of the strong base site density is also observed in the IR spectra taken at similar CO_2 desorption temperatures. For instance, after evacuation at 573 K, mostly unidentate carbonates remain on the surface of the Cs/MgO sample (not shown) in contrast to the prevalent presence of bidentate carbonates on pure MgO and Li/MgO (Fig. 2). From the above IR and TPD results, it can be concluded that the alkali promotion increases not only the total number of basic sites of pure MgO, but also its average basic strength.

3.2. Elimination reactions in 2-propanol decomposition

Decomposition of 2-propanol was used to study the acid–base active site requirements for elimination reactions on alkali-promoted MgO catalysts.

In previous work [25,28], we have studied the decomposition of ethanol and 1-propanol on Mg–Al oxides to ascertain the role of the surface acid–base properties on elimination reactions of primary alcohols. We concluded that on acidic Al-rich Mg–Al oxide samples, primary alcohols dehydrate on acid–base pair sites via a concerted E_2 mechanism, whereas on basic Mg-rich samples the reaction proceeds also on acid–base pairs but through an E_{1cB} anionic mechanism. On the other hand, dehydrogenation of primary alcohols would proceed predominantly on acid–base pairs of Mg-rich Mg–Al mixed oxides through the formation of carbanion intermediates. On Mg-based catalysts, we also investigated by H_2–D_2 steady state equilibration reactions [28], the activation of the H–H bond which is kinetically related to the C–H bond and we found that pure MgO heterolytically dissociates H_2 at measurable rates at reaction temperatures as low as 298 K.

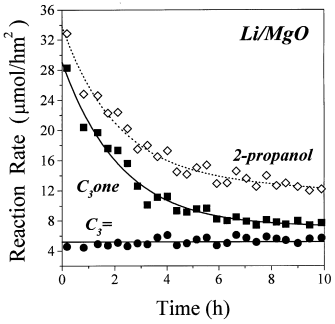

Fig. 4. 2-Propanol decomposition reactions at 533 K. 2-Propanol reaction rate and C_3= and C_3one formation rates as a function of time-on-stream for Li/MgO catalyst.

On MgO-based catalysts, 2-propanol is dehydrogenated to acetone (C_3one) and dehydrated to propylene (C_3=) with zero-order reactions [10,21]. Fig. 4 illustrates the time-on-stream behavior of the Li/MgO catalyst at 533 K during the 2-propanol conversion reactions. Similar qualitative curves representing the activity decay were obtained for the other catalysts. The total activity and the C_3one formation rate decreased with time-on-stream on both MgO and A/MgO samples, but the C_3= formation rate decay was in all cases negligible. Initial reaction rates were measured by extrapolating the activity vs. time curves to zero time. Table 2 presents the obtained values of the total conversion rate (r_0) as well as of the dehydrogenation (C_3one formation) and dehydration rates (C_3= formation). The r_0 values on A/MgO catalysts are higher than on MgO (4.14 μmol/h m^2), thereby revealing that the promoter addition increases the MgO activity for 2-propanol decomposition. The Li/MgO sample exhibits the highest total activity (33.74 μmol/h m^2). From Tables 1 and 2 it is inferred that r_0 on MgO and A/MgO samples increases linearly with the density of basic sites measured by TPD of CO_2. This proportionality between r_0 and n_{CO_2} suggests that rate-limiting steps in the reaction mechanism for

Table 2
Decomposition of 2-propanol on A/MgO and MgO catalysts[a]

Catalyst	2-Propanol conversion (%)	2-Propanol conversion rate (μmol/h m^2)	Formation rate (μmol/h m^2)	
			C_3one	C_3=
MgO	1.58	4.14	2.89	1.25
Li/MgO	13.84	33.74	28.65	4.62
Na/MgO	2.79	9.71	6.64	3.07
K/MgO	5.61	22.08	14.18	7.90
Cs/MgO	6.16	28.76	15.85	12.91

[a] $T = 533$ K, $P = 100$ kPa, N_2/2-propanol = 15, WHSV = 2 h^{-1}.

2-propanol conversion are catalyzed by surface base sites.

Results of Table 2 show that on MgO and A/MgO catalysts, 2-propanol is predominantly dehydrogenated to C_3one and, to a less extent, dehydrated to C_3=. No ether or condensation products were detected. On all the catalysts, the selectivity to acetone was higher than 55%, but the product distribution of 2-propanol decomposition depended on the active site density and strength. The Li/MgO catalyst contains the highest concentration of medium-strength base sites and forms 86% of acetone, whereas on Cs/MgO the high-strength base sites are predominant and the propylene selectivity reaches 45%. The plots of Fig. 5 show that the acetone formation rate effectively increases with increasing the density of medium-strength base sites (M-peak); in contrast, the olefin formation is favored on catalysts containing an enhanced contribution of high-strength basic sites (H-peak). These results can be interpreted by assuming that rate-limiting steps of the dehydrogenation and dehydration reactions are catalyzed by Mg(A)–O pairs of intermediate basic strength and by strongly basic O^{2-} sites, respectively.

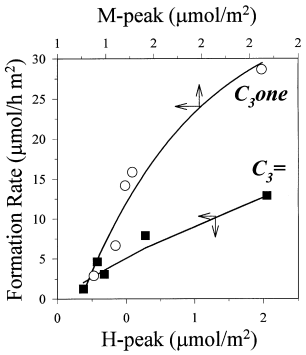

Fig. 5. C_3= and C_3one formation rates as a function of the density of high-strength (H-peak) and medium-strength (M-peak) base sites, respectively.

The assumption that 2-propanol dehydrogenation and dehydration reactions occur on different basic active sites is supported by the results in Fig. 4, which show that the two reactions deactivate following different activity decay patterns. In a previous work [29], we studied the deactivation of alkali-promoted MgO catalysts during the self-condensation of acetone and we found that the formation of α,β-unsaturated condensed compounds by acetone oligomerization on acid–base pairs are responsible for coke formation and blockage of active sites. Similarly, the acetone produced by 2-propanol dehydrogenation may condense before desorption and form α,β-unsaturated compounds that remain adsorbed on the catalyst surface and are not detected in the products. Formation of these α,β-unsaturated compounds on the same acid–base pairs involved in the rate-determining step of 2-propanol dehydrogenation to acetone explains the acetone formation rate decay observed in Fig. 4. The absence of noticeable deactivation during C_3= formation may be explained by considering that 2-propanol dehydration to propylene is catalyzed by isolated O^{2-} sites and will not be affected then by the simultaneous formation and stabilization of acetone oligomers on Mg(A)–O pair sites.

The present catalytic results and previous work [15,25] allow us to propose that the decomposition of 2-propanol occurs via two parallel reactions proceeding both through an E_{1cB}-like elimination mechanism, which involves a common alkoxide intermediate (Fig. 6). The reaction sequence in Fig. 6 involves the initial dissociative adsorption of 2-propanol on weak-Lewis-acid–strong-Brönsted-base pairs (Mg(A)–O) which break the OH bond forming a surface alkoxide intermediate. The subsequent abstraction of H^{α} or H^{β} from the 2-propoxide anion intermediate leads to ketone or olefin formation, respectively. Predominant formation of either ketone or olefin will depend, therefore, on the relative acidity of H^{α} and H^{β} protons and on the acid–base properties of the catalytic material. Our results of Fig. 5 suggest that on alkali-promoted MgO catalysts the H^{β} abstraction from the 2-propoxy intermediate to

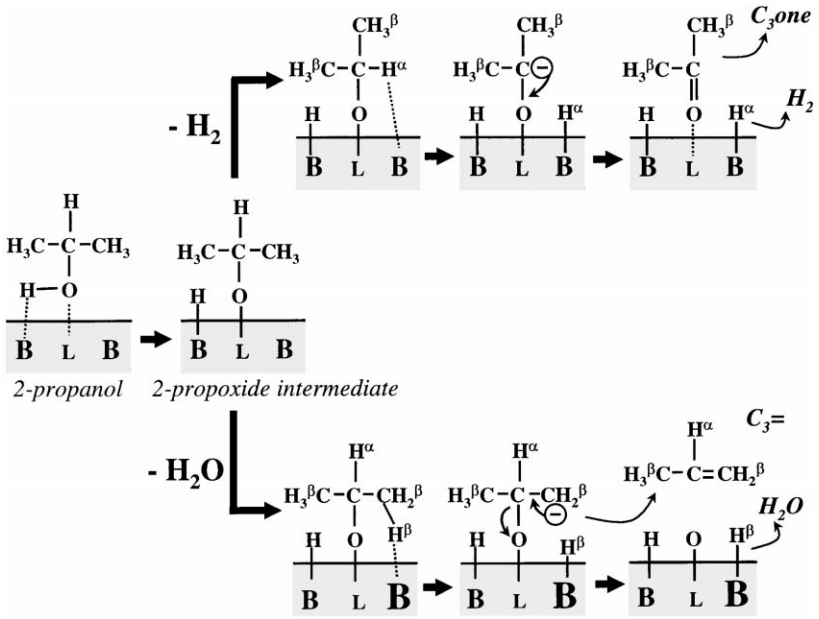

Fig. 6. Formation of C_3= and C_3one on MgO and A/MgO catalysts via base-catalyzed E_{1cB} mechanisms. L: weak Lewis acid site (A^+ or Mg^{2+} cations); B: medium-strength Brönsted base sites (combined oxygen in A–O or Mg–O pairs); **B**: high-strength Brönsted base sites (isolated O^{2-}).

form C_3= requires stronger basic sites than the H^α abstraction leading to C_3one. The different basicity requirements for both elimination reactions may be explained by the energetic differences between H^α and H^β abstraction. Waugh et al. [30] studied the temperature-programmed decomposition of 2-propanol on ZnO and found that the activation energy for α-hydrogen abstraction from the 2-propoxide intermediate is lower than for H^β abstraction. On the other hand, Canesson and Blanchard [31] reported that the more substituted the C^α in the alcohol, the stronger the basic site needed for the H^β abstraction from the alcohol molecule.

In order to confirm that the β-proton abstraction occurs on stronger basic sites, we measured the activation energy (E_a) for C_3= formation on MgO, Li/MgO and Cs/MgO samples in the temperature range 513–553 K. Results are shown in Fig. 7 as a function of the relative concentration of high-strength base sites. It is observed that the E_a value decreases with increasing the relative concentration of high-strength base sites. Abstraction of the H^β is relatively easier on Cs/MgO catalyst where the high-strength base sites are dominant, whereas the highest activation energy was measured on Li/MgO which presents the lowest average basic strength. Similarly, Gervasini et al. [15] found that the activation energy for C_3= formation on 0.23 mol% Li/MgO (E_a ∼31 kcal/mol) is higher than on pure MgO (E_a ∼29 kcal/mol).

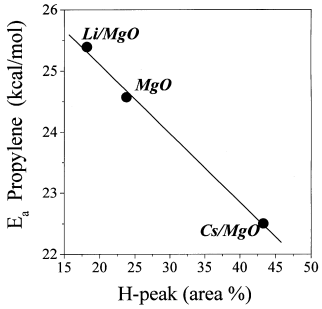

Fig. 7. Activation energy for C_3= formation on MgO and A/MgO catalysts as a function of the relative concentration of high-strength base sites (H-peak).

In summary, we propose that the 2-propanol decomposition on alkali-promoted MgO occurs through the reaction mechanism of Fig. 6. The medium-strength basic sites are predominant on MgO and A/MgO catalysts and preferentially catalyze the rate-determining step of the energetically easier H^{α} abstraction from adsorbed 2-propoxide forming a carbanion intermediate that finally leads to acetone. In contrast, the 2-propanol dehydration to propylene requires strongly basic O^{2-} species to abstract the H^{β} from the 2-propoxide intermediate. In the reaction sequence of Fig. 6, the role of the Lewis acid centers is limited to the stabilization of the ionic intermediates.

4. Conclusions

The basic properties of MgO and alkali-promoted MgO depend on the relative concentration of surface sites of different chemical nature and strength, i.e., OH groups, oxygen in Mg–O pairs and isolated O^{2-} anions. Addition to magnesium oxide of alkaline metal ions increases the total basic site density. The promoter also modifies the strength of basic sites on MgO: the stronger the electrodonating properties of the promoter, the higher the generation of strong basic sites.

The decomposition of 2-propanol on MgO-based catalysts occurs via two parallel elimination pathways leading to acetone and propylene, respectively. The alcohol dehydrogenation to acetone is the predominant reaction and proceeds via an E_{1cB}-like mechanism catalyzed by medium-strength basic sites. In contrast, propylene formation is catalyzed by strong basic sites and, consequently, is favored on alkali-modified MgO catalysts presenting enhanced electrodonating properties.

The activity for 2-propanol decomposition on alkali-promoted MgO samples is higher than on MgO and essentially reflects the generation of medium-strength basic sites, which are effective for the formation of initial alkoxide intermediates via the OH bond rupture from the adsorbed alcohol. Decomposition of 2-propanol is a simple and useful reaction to probe the effect of the catalyst acid–base properties on elimination reactions.

Acknowledgements

The authors thank the Universidad Nacional del Litoral, Santa Fe, Argentina and CONICET (Argentina) for the financial support of this work. The authors also thank H. Cabral and T. Garetto for their technical assistance.

References

[1] H. Hattori, in: Proceedings of the Third International Symposium on Heterogeneous Catalysis and Fine Chemicals, Poitiers, 1993, p. L19.
[2] G. Zhang, H. Hattori, K. Tanabe, Appl. Catal. 36 (1988) 198.
[3] J.I. Di Cosimo, V.K. Díez, C.R. Apesteguía, Appl. Catal. 137 (1996) 149.
[4] A. Corma, S. Iborra, J. Primo, F. Rey, Appl. Catal. 114 (1994) 215.
[5] M. Xu, M.J.L. Ginés, A.-M. Hilmen, B.L. Stephens, E. Iglesia, J. Catal. 171 (1997) 130.
[6] H. Kurokawa, T. Kato, T. Kuwabara, W. Ueda, Y. Morikawa, Y. Moro-Oka, T. Ikawa, J. Catal. 126 (1990) 208.
[7] S. Malinowski, in: B. Imelik, et al. (Eds.), Catalysis by Acids and Bases, Elsevier, Amsterdam, 1985, p. 57.
[8] K. Tanabe, M. Misono, Y. Ono, H. Hattori (Eds.), New Solid Acids and Bases, Kodansha/Elsevier, Tokyo/Amsterdam, 1989, pp. 260–267.
[9] M. Ai, J. Catal. 40 (1975) 318.
[10] A. Gervasini, A. Auroux, J. Catal. 131 (1991) 190.
[11] H. Lauron-Pernot, F. Luck, J.M. Popa, Appl. Catal. 78 (1991) 213.
[12] C. Lahousse, J. Bachelier, J.C. Lavalley, H. Lauron Pernot, A.M. Le Govic, J. Mol. Catal. 87 (1994) 329.
[13] B. Davis, in: M. Che, G.C. Bond (Eds.), Adsorption and Catalysis on Oxide Surfaces, Elsevier, Amsterdam, 1985, p. 309.
[14] C.P. Bezouhanova, M.A. Al-Zihari, Catal. Lett. 11 (1991) 245.
[15] A. Gervasini, J. Fenyvesi, A. Auroux, Catal. Lett. 43 (1997) 219.
[16] S.V. Bordawekar, E.J. Doskocil, R. Davis, Catal. Lett. 44 (1997) 193.
[17] Z.G. Szabó, B. Jóvér, R. Ochmacht, J. Catal. 39 (1975) 225.
[18] R.T. Sanderson, in: Chemical Bonds and Bond Energy, 2nd Edition, Academic Press, New York, 1976.
[19] A. Auroux, A. Gervasini, J. Phys. Chem. 94 (1990) 6371.
[20] R. Philipp, K. Fujimoto, J. Phys. Chem. 96 (1992) 9035.
[21] A.L. McKenzie, C.T. Fischell, R.J. Davis, J. Catal. 138 (1992) 547.
[22] H. Kurokawa, W. Ueda, Y. Morikawa, Y. Moro-Oka, T. Ikawa, in: K. Tanabe, H. Hattori, T. Yamaguchi, T. Tanaka (Eds.), Acid–Base Catalysis, Kodansha, Tokyo, 1989, p. 93.
[23] T. Kanno, M. Kobayashi, in: M. Misono, Y. Ono (Eds.), Acid–Base Catalysts II, Kodansha/Elsevier, Tokyo/Amsterdam, 1994, pp. 207–211.

[24] J. Kijenski, S. Malinowski, J. Chem. Soc., Faraday Trans. 74 (1978) 250.
[25] J.I. Di Cosimo, V.K. Díez, M. Xu, E. Iglesia, C.R. Apesteguía, J. Catal. 178 (1998) 499.
[26] C. Morterra, G. Ghiotti, F. Boccuzzi, S. Coluccia, J. Catal. 51 (1978) 299.
[27] J.V. Evans, T.L. Whateley, Trans. Faraday Soc. 63 (1967) 2769.
[28] J.I. Di Cosimo, C.R. Apesteguía, M.J.L. Ginés, E. Iglesia, J. Catal. 190 (2000) 261.
[29] J.I. Di Cosimo, C.R. Apesteguía, J. Mol. Catal. 130 (1998) 177.
[30] K.C. Waugh, M. Bowker, R.W. Petts, H.D. Vanderwell, J. O'Malley, Appl. Catal. 25 (1986) 121.
[31] P. Canesson, M. Blanchard, J. Catal. 42 (1976) 205.